Wavelength Sampling and Quantizing Optical ADC Based on Long-period Waveguide Grating Filter

Qianshu Zhang
Dept. of Physics & Electronic Information
China West Normal University
Nanchong, China
qshzhang@uestc.edu.cn

Yong Liu, Shangjian Zhang, Heping Li, Yongzhi Liu
Opto-Electronic Information School
University of Electronic Science & Technology of China
Chengdu, China

***Abstract*—We present a novel optical wavelength sampling and quantizing method that can be used for photonic analog-to-digital converters. The wavelength sampling is realized by using a high-speed optical tunable filter. The tunable filter has long-period-waveguide-grating structure, and is controlled by an analog electronic signal. The output wavelength of the optical filter is determined by the amplitude of the analog electronic signal. Different amplitude leads to the optical filter outputting different wavelength. An arrayed waveguide grating separates the different wavelength into different spatial channel to complete wavelength quantizing function. At the output of the spatial channels, a detector array is used to realize the coding function. The utilization of wavelength sampling and quantizing allows the analog-to-digital converter to achieve high resolution because the sampling and quantizing are carried out in the wavelength domain, which is immune to the intensity noise and disturbance. The limits on sampling rate and quantization resolution are investigated in detail. The analysis results are shown that our analog-to-digital converter scheme is promising to achieve high-resolution of 8 bits at the sampling rate of 10 GS/s.**

Keywords-photonic analog-to-digital conversion; wavelength sampling; wavelength quantizing; electro-optical tunable filter.

I. INTRODUCTION

Nowadays radar and satellite communications systems need high-speed analog-to-digital converters (ADCs) for signal processing [1]. Electronic ADCs have some difficulties for achieving high-speed operation due to the problems of the aperture jitter, thermal noise and ambiguity induced by the electronic component [2]. Photonic ADCs schemes are proposed and investigated to overcome the inherently limitation of electronic ADCs [3]. In general, photonic ADCs can be classified into four categories: photonic assisted [4-6], photonic sampled [7-9], photonic quantized [10-12], photonic sampled and quantized [13, 14]. However, Most of the schemes take the intensity or phase of light as signal carrier to realize the ADC function. The amplitude and phase noise in the system will degrade the resolution of photonic ADCs. In fact, the current photonic ADCs can achieve high operating speed but the resolution is relatively low, which limits the application.

In this paper, we present a novel optical wavelength sampling and quantizing method that can be used for photonic analog-to-digital conversion. This photonic ADC can achieve high resolution because the sampling and quantizing is carried out in the wavelength domain, which is immune to the intensity noise and phase noise. The operation principle of the proposed scheme is described. The performance of the wavelength sampling and quantizing ADC is analysis in theory. The analysis results are shown that our ADC is promising to achieve high-resolution of 8 bits at the sampling rate of 10 GS/s.

This work was supported by the National Nature Science Foundation of China (No. 60736038, 60907008, 60925019), NCET Program (No. NCET-07-0152), Sichuan Scientific Funds for Young Researchers (No. 08ZQ026-012) and Education Ministry Funds for New Teachers (No. 200806141102).

II. CONCEPT OF WAVELENGTH SAMPLING AND QUANTIZING ADC

The configuration of the wavelength sampling and quantizing (WSWQ) ADC is depicted in Fig. 1, which is made from a pulsed laser, a high-speed electro-optical tunable filter, an arrayed waveguide grating (AWG) and a spatial array of detectors.

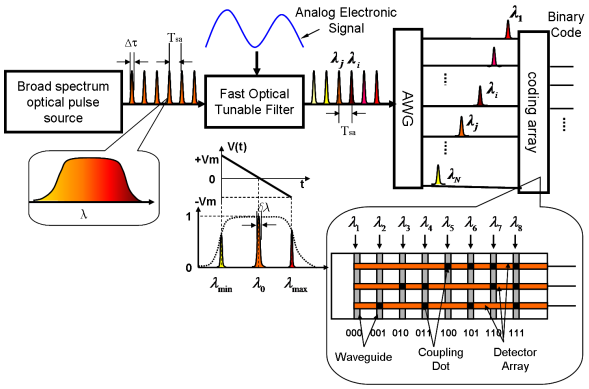

Figure 1. The scheme of wavelength sampling and quantizing ADC

The pulsed laser emits optical sampling pulses with low-jitter and broadband optical spectrum. The sampling optical pulses are fed into the optical tunable filter, and then the wavelength samples of signal output from the filter. The center wavelength of the optical samples is determined by the amplitude of the applied electronic voltage. In our scheme, the analog electronic signal drives the optical tunable filter, selecting the output wavelength of the filter. Therefore, the different amplitude of the electronic signal leads to a different wavelength output. The filter output is sent into the AWG, where the sampled pulses with different wavelength are spatially separated into different channels. Thus the wavelength sampling and quantizing are realized. At the output of the channels, a detector array forms spatial coding function, as shown in Fig.1.

978-1-4244-4964-4/10/$25.00 ©2010 IEEE

A. *Wavelength Sampling Based on High-speed optical tunable filter*

The crucial component in our scheme is the high-speed optical tunable filter. To meet the requirements of the ADC, the filter needs to have fast tuning speed, large tuning range and narrow passband. We use long-period waveguide grating (LPWG) structure to realize such an optical tunable filter, as shown in Fig.2, which has been analyzed detailed in [15]. The analysis results show that the filter can realize high-speed linearity wavelength tuning within 30 nm wavelength range with a narrow passband of 0.8 nm.

As shown in Fig. 2, the EO tunable LPWG filter consists of two parallel identical single-mode waveguides named core 1 and core 2, respectively. The two waveguides are both buried in the same cladding and two LPWGs are identically fabricated on the surface of the two waveguides. Two tuning electrodes are manufactured on the cladding layer and located just over the two LPWGs for wavelength tuning.

A wavelength selectivity coupling between the guided modes of the two waveguides and the cladding mode can be aroused by the LPWGs. The wavelength selectivity of the coupling derives from the phase-matching condition of the LPWGs, which is

$$\lambda_0 = \left(N_{co} - N_{cl}\right)\Lambda, \tag{1}$$

where N_{co} and N_{cl} are the effective indices of the guided modes and the cladding modes, Λ is the period of LPWG, λ_0 is named static resonance wavelength.

Owing to the wavelength selectivity coupling, when wide spectrum light is launched into core 1, a narrow band of light with center wavelength of λ_0 will be filtered out from core 1 and coupled into core 2. Therefore, we can get a band-pass filtering result from the end of core 2 and band-rejection filtering result from the end of core 1, as shown in Fig.2.

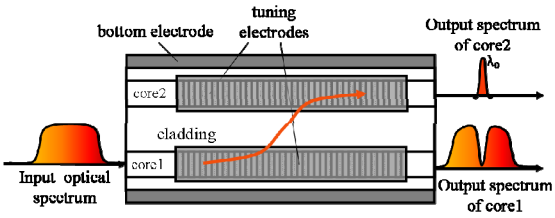

Figure 2. The principle of the EO tunable filter based on LPWG

If we apply voltage to the tuning electrodes to change the effective index N_{co} of guided modes, the resonance wavelength is changed accordingly:

$$\lambda_0' = \Delta N_{co}\Lambda + \lambda_0 = KV_{in} + \lambda_0, \tag{2}$$

where $K = -\left(\frac{1}{2} n_{co}^3 \gamma_{33} \frac{\Lambda}{D}\right)$ is defined as the wavelength tuning sensitivity, n_{co} is the material index of waveguide, γ_{33} is the EO coefficient, V_{in} is the applied tuning voltage, and D is the total thickness between the upper and bottom electrodes.

According to (2), when the waveguide material parameters and the structure parameters of the filter are set, we can get a linear wavelength tuning filter. When the waveguide cores are made from IPC-E/polysulfone with refractive index n_{co}=1.67 and electro-optic coefficient γ_{33}=55 pm/V after poled [16], the thickness D is equal to 4 μm, the period of the LPWG Λ is equal to 31.131 μm, and the static resonance wavelength λ_0 is set as 1545 nm, we can get the wavelength tuning curve of the filter. As shown in Fig.3(a), when the tuning voltage is increased from -15 to +15 volts, the resonance wavelength will be declined linearly from 1530 nm to 1560 nm. The linearity property of the filter in wavelength tuning suggests that using the EO tunable LPWG filter for wavelength sampling can avoid sampling distortion occurred in sampling operation.

Fig.3(b) shows the simulation results of wavelength sampling. When an stepped voltage signal applies on the tuning electrodes of the EO tunable filter, a narrow band optical pulse will output from the output port of core 2, as shown in Fig.3(b). The center wavelength of the output optical pulse is one-to-one correspondence with the magnitude of tuning voltage. Thus wavelength sampling operation is realized.

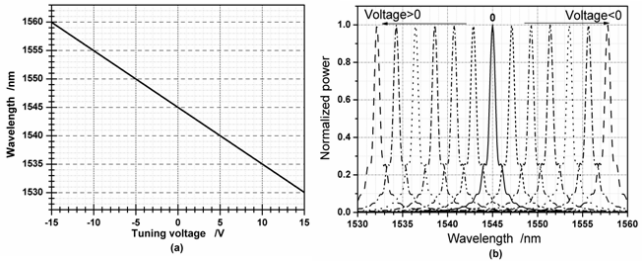

Figure 3. The characteristcs of the EO tunable filter. (a) is the curve of wavelength tuning; (b) is the simulation result of wavelength sampling.

B. *Wavelength Quantization Based on AWG*

Since the AWG can separate light of differing wavelength and output them from different port, we use it to separate the sampled optical pulse spatially and quantize them in our optical ADC scheme.

According to (2), the center wavelength of sampled optical pulse is one-to-one correspondence with the magnitude of tuning voltage. If the operating wavelength range of the EO tunable filter is designed to coincide with the AWG's, the output port number can be given by:

$$n = \text{int}\left(\frac{\lambda_0' - \lambda_{\min}}{\Delta\lambda_{ch}}\right) = \text{int}\left(\frac{KV_{in} + \lambda_0 - \lambda_{\min}}{\Delta\lambda_{ch}}\right), \tag{3}$$

where $\Delta\lambda_{ch}$ is the channel spacing of AWG, λ_{min} is the minimum in the filter's operation wavelength range. Equation (3) indicates that one output port of AWG, numbered n, is also one-to-one correspondence with one tuning voltage range. If the AWG has 2^N channels, the tuning voltage is also divided into 2^N corresponding quantization levels, and then each of the output ports represents one quantization level. If the AWG's output ports are encoded in advance by N bits binary codes to represent the quantization voltage level, we can use AWG for wavelength quantizing in our ADC scheme.

For example, as shown in Fig.4, when a signal voltage of +Vm volt applies on the filter's tuning electrodes, a sampled optical pulse with the center wavelength of λ_{min} will be filtered out and fed into an AWG with 2^6 channels. Subsequently, it will be output from the No.1 port of the AWG, which represents the code "111111". Thus, the quantization process is realized.

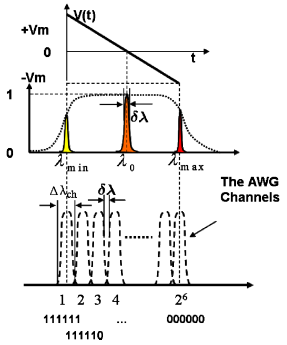

Figure 4. The scheme of wavelength quantization with AWG

The practical quantization resolution of our optical ADC scheme is determined by the operation wavelength range of filter and the channel spacing of AWG. The quantization resolutions in bits can be expressed as:

$$N = \log_2\left(\frac{\lambda_{\max} - \lambda_{\min}}{\Delta\lambda_{ch}}\right), \tag{4}$$

where λ_{max} is the maximum in the filter's operation wavelength range. We can estimate the quantization resolutions by the numbers of AWG output channel. If the AWG has 64 output channels within its operation wavelength range, we can get 64 quantization levels and 6 bits quantization resolutions.

III. Performance of Wavelength Sampling and Quantizing ADC

A. Sampling Rate

Since one sampling optical pulse passes through the filter and obtains one wavelength sample, the sampling rate is equal to the light pulse repetition rate. A series of light pulses with repetition rate of 150 GHz obtained by the time-interleaved technology already has been reported in [17]. Therefore, the wavelength sampling ADC of our scheme has potential to obtain high-speed sampling at the rate of 150 GS/s.

B. Effective number of bits (ENOB)

In order to evaluate the highest achievable ENOB of our WQWS optical ADC scheme, we will discuss the limits on ENOB introduced by the sampling optical pulse, as follows.

For an ideal optical ADC, the resolution is only limited by the quantization noise. The square-root of the quantization noise power and the resolution in bits of the ideal optical ADC are given, respectively, by [1]:

$$\sigma_q = Q/\sqrt{12}, \tag{5}$$

$$N = \left(SNR_q - 1.76\right)/6.02, \tag{6}$$

where Q is the size of the elementary quantization step and equal to $2^{-N}V_{FS}$, V_{FS} is the full-scale voltage range, and SNR_q is the ratio of the root-mean-square signal amplitude to the square-root of the quantization noise power.

Because many additional error mechanisms are also present in a practical optical ADC, such as amplitude noise, timing jitter and the finite width of the sampling optical pulse, the resolution determined by (6) is the upper limit of quantization resolution which a physical optical ADC can get. In order to obtain the highest ENOB, the square-root of the noise power induced by amplitude noise, timing jitter and width of the optical sampling pulse, respectively, should be smaller than that of the quantization noise. So taking the quantization noise as criterion, we can get the limits on ENOB of our optical ADC scheme.

Since the sampling and quantizing process of our WSWQ ADC scheme is carried out in the wavelength domain, which is immune to the amplitude noise and phase noise, only the timing jitter and the width of the sampling optical pulse degrades the ENOB of our optical ADC scheme.

1) Timing jitter

For a sinusoidal signal with amplitude of A and frequency of $f_{sa}/2$, where f_{sa} is the sampling rate, the sample error induced by the timing jitter Δt is given by:

$$\begin{aligned}\Delta V &= A\sin\left[\pi f_{sa}\left(t-\Delta t\right)\right] - A\sin\left(\pi f_{sa} t\right)\\ &\approx A\pi f_{sa}\Delta t\cos\left(\pi f_{sa} t\right)\end{aligned} \tag{7}$$

In general situation, the timing jitter of the sampling optical pulse is an uncorrelated Gaussian random process and has a standard deviation of σ_j^2. Since the sine wave is sampled at random within its period, the standard deviation of ΔV is given by:

$$\sigma_V^2 = \frac{1}{2}\left(A\pi f_{sa}\sigma_j\right)^2 \tag{8}$$

Assumption that the error induced by the timing jitter is equal to the quantization noise power, we can get the ENOB limited by the timing jitter as shown below:

$$N_j = \log_2\left(\frac{1}{\sqrt{3}\pi f_{sa}\sigma_j}\right) + \frac{1}{2} \tag{9}$$

Fig.5(a) shows the limits on the ENOB of our WSWQ optical ADC induced by the timing jitter. As shown in Fig.5 (a), the sampling rate and the ENOB are both declined with the increasing of timing jitter. For achieving the ENOB of 10 bits at the sampling rate of 10 GS/s, the timing jitter is required smaller than 25.4 fs.

2) Finite sampling pulse width

If a Gaussian optical pulse train samples a sinusoidal signal with amplitude of A and frequency of $f_{sa}/2$, the sample error induced by the sampling pulse width T_p is given by:

$$\Delta V = A\sin\left(\pi f_{sa} t\right) - \frac{A}{\sqrt{2\pi}\sigma_p}\int \sin\left(\pi f_{sa} t_1\right)\exp\left[\frac{-\left(t_1 - t\right)^2}{2\sigma_p^2}\right]dt_1, \quad (10)$$

where σ_p is the square-root width of Gaussian optical pulse, the integral is carried out on one sampling period. If the duty cycle of the sampling optical pulse is smaller than 10 %, we can approximate the integral limits by -∞ to +∞. Since the sine wave is sampled at random in its period, the standard deviation of ΔV is given by:

$$\sigma_V^2 = \frac{A^2}{2}\left\{1 - \exp\left[\frac{-\left(\pi f_{sa}\sigma_p\right)^2}{2}\right]\right\}^2, \quad (11)$$

Substituting the optical pulse's FWHM $T_p = \sqrt{8\ln 2}\sigma_p$ into (11), we can get the ENOB limited by the width of sampling optical pulse as following:

$$N_w = \log_2\left(\frac{1}{f_{sa}T_p}\right) = \log_2\left(\frac{T_{sa}}{T_p}\right) \quad (12)$$

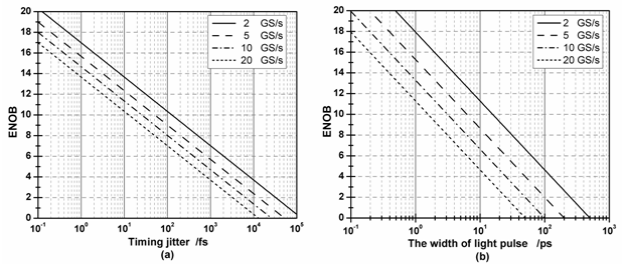

Figure 5. The limits on the ENOB of WSWQ optical ADC induced by (a) timing jitter and (b) finite width of the optical pulse, respectively.

The ENOB of our WSWQ optical ADC limited by the width of sampling optical pulse is depicted in Fig. 5(b). As shown in Fig. 5(b), the sampling rate and the ENOB are both degraded with the increasing in width of the sampling pulse. For achieving the ENOB of 10 bits at sampling rate of 10 GS/s, the width of the sampling pulse is required smaller than 3.125 ps.

According to (9) and (12), an optical pulse train with pulse repetition rate of 10 GHz, timing jitter smaller than 102 fs and pulse width smaller than 6.25 ps is required for an WSWQ optical ADC to obtain the ENOB of 8 bits at sampling rate of 10 GS/s. The optical pulse train, as mentioned above, can be generated by current mode-locked laser (MLL). For example, a state-of-the-art of MLL (MLL1550, u^{2}t photonic), which is characteristic of 10.9-GHz repetition rate and 100-fs timing jitter and 1.3-ps optical pulse width, has already been merchandized. Taking it as the source of our WSWQ ADC, we can obtain an optical ADC with the ENOB of 8 bits at sampling rate of 10 GS/s. If the timing jitter is decreased to 25.4 fs, the ENOB of our ADC scheme can be improved to 10 bits. Therefore, our WSWQ optical ADC scheme is promising for high-resolution and high-speed photonic ADC.

IV. CONCLUSION

We present a novel wavelength sampling and quantizing method that can be used for photonic ADC, which has an advantage for achieving high-resolution operation at fast sampling rate. We investigate the performance of the wavelength sampling and quantizing ADC theoretically. The analysis results show that the photonic ADC is promising to obtain ENOB of 8 bits at the sampling rate of 10 GS/s.

REFERENCES

[1] R. H. Walden, "Analog-to-digital converter survey and analysis," IEEE J. Sel. Areas Comm. 17, 539-550, 1999.

[2] R. H. Walden, "Analog-to-digital conversion in the early 21st century," presented at the International Microwave Symposium, Honolulu, Hawaii, 3-8, June, 2007.

[3] G. C. Valley, "Photonic analog-to-digital converters," Opt. Express 15, 1955-1982, 2007.

[4] F. J. Leonberger and P. Moulton, "High-speed InP optoelectronic switch," Appl. Phys. Lett. 35, 712-714, 1979.

[5] R. F. Pease, K. Ioakeimidi, R. Aldana, et al. "Photoelectronic analog-to-digital conversion using miniature electron optics: Basic design considerations," J. Vac. Sci. Technol. 21, 2826-2829, 2003.

[6] K. Ioakeimidi, R. F. Leheny, S. Gradinaru, et al. "Photoelectronic analog-to-digital conversion: sampling and quantizing at 100 Gs/s," IEEE Trans. Microwave Theory and Tech. 53, 336-342, 2005.

[7] P. W. Juodawlkis, J. C. Twichell, G. E. Betts, et al. "Optically sampled analog-to-digital converters," IEEE Trans.Microwave Theory Tech. 49, 1840-1853, 2001.

[8] J. C. Twichell, J. L. Wasserman, P. W. Juodawlkis, et al. "High-linearity 208-MS/s photonic analog-to-digital converter using 1-to-4 optical time-division demultiplexers," IEEE Photonic Technol. Lett. 13, 714-716, July 2001.

[9] R. C. Williamson, P. W. Juodawlkis, et al. "Effects of crosstalk in demultiplexers for photonic analog-to-digital converters," J. Lightwave Technol. 19, 230-236, 2001.

[10] H. Zmuda, "Analog-to-digital conversion using high-speed photonic processing," Proc. SPIE 4490, 84-95, 2001.

[11] H. Zmuda, M. J. Hayduk, R. J. Bussjager, et al "Wavelength-based analog-to-digital conversion," Proc. SPIE 4547, 134-145, 2002.

[12] E. N. Toughlian and H. Zmuda, "A photonic wideband analog to digital converter," International Topical Meeting on Microwave Photonics 2000, 248-250, 2000.

[13] H. F. Taylor, "An electro-optic analog-to-digital converter," Proc. IEEE 63, 1524-1525, 1975.

[14] R. A. Becker, C. E. Woodward, F. J. Leonberger, and R. C. Williamson, "Wideband electrooptic guidedwave analog-to-digital converters," Proc. IEEE 72, 802-819, 1984.

[15] Qianshu Zhang, Yongzhi Liu, Jinkun Liao, Rongguo Lu, Lin Huang, Xionggui Tang, et al.,"Design and Simulation of a Narrow Passband Electro-Optical Tunable Filter with Band-pass and Band-rejection Output" Journal of Infrared, Millimeter, and Terahertz Waves, Vol.30, No.9: 959-968, 2009.

[16] S. M. Garner, J. S. Cites, M. He, et al. "Polysulfone as an electro-optic polymer host material," Appl. Physics Lett., 84, 1049-1051, 2004.

[17] A. S. Bhushan, F. Coppinger, B. Jalali, S. Wang and H. F.Fetterman, 150 Gsample/s wavelength division sampler with time-stretched output, Electron. Lett.,34:474-475,1998

.